Int J Adv Manuf Technol (2015) 81:1809–1816
DOI 10.1007/s00170-015-7271-3

ORIGINAL ARTICLE

Effect of feeding length on deforming behavior of Ti-3Al-2.5 V tubular components prepared by tube gas forming at elevated temperature

Gang Liu [1,2] · Yong Wu [1] · Dongjun Wang [1] · Shijian Yuan [1,2]

Received: 21 January 2015 / Accepted: 4 May 2015 / Published online: 28 May 2015

Abstract In order to investigate the deforming behavior of the tubular components with a large expansion ratio fabricated by tube gas forming technique, the Ti-3Al-2.5 V tubular components with 50 % expansion ratio were studied under the forming conditions of internal pressure and axial feeding at 800 °C. Through thickness measurements, EBSD and tensile tests, the effects of axial feeding on deforming behaviors, such as thickness distribution, microstructure, and mechanical properties of Ti-3Al-2.5 V tubular components, were investigated in details. The results showed that the average thinning ratio of the bulging area could be reduced significantly and the thickness distribution of the workpiece was more uniform with increasing of the feeding. Feeding length influenced the microstructure and strength of components. When the axial feeding ratio (actual feeding length/theoretical feeding length) was 56 %, the component had even higher tensile strength than the original tube because of the grain refinement. If the axial feeding was excessive large, the grain size became adversely coarser, which in turn reduced the tensile strength. These investigations illustrated that tube gas forming under high pressure had potential for fabricating complicated shaped titanium alloy tubular components by reasonably designing and controlling the deforming process.

Keywords Tube gas forming · Axial feeding · Tubular components · Thickness distribution · Titanium alloy · EBSD

✉ Gang Liu
gliu@hit.edu.cn

[1] School of Materials Science and Engineering, Harbin Institute of Technology, Harbin 150001, China

[2] National Key Laboratory for Precision Hot Processing of Metals, Harbin Institute of Technology, Harbin 150001, China

1 Introduction

Hydroforming is considered as one of novel forming processes to produce complicated shaped components of metal materials at room temperature. Among them, tube hydroforming also has other advantages, such as excellent forming ability, low cost, and uniform thickness distribution. To improve the formability of workpieces with low ductility and strong deforming resistance at room temperature, warm and hot forming techniques are developed. Geiger [1] and Yuan [2] developed warm hydroforming systems with maximal heating temperature of 315 °C to form magnesium tubular components. However, the heating temperature of normal warm tube hydroforming method is usually below 350 °C, which is difficult to produce complicated shaped products with heat-resistant and hard-to-deform materials, e.g., Ti alloy.

In recent years, quick plastic forming (QPF) has been developed by US car manufacturers as a hot blow forming process, which is capable to produce mass aluminum panels [3, 4]. For aluminum and magnesium tubular components, hot metal gas forming (HMGF) with higher forming temperature has also been developed using low internal pressure gas, which has drawn much attention due to the advantage of high efficiency [5, 6]. Wu [7] reported the HMGF mechanism of Mg-alloy tubes. Kim [8] fabricated an aluminum suspension component by HMGF at 520 °C under a constant gas pressure of 7 MPa. Furthermore, the company Heatform Gmbh [9] developed the hot expansion air forming technology to produce the tubular components at elevated temperatures. Maeno [10–12] studied the aluminium alloy tube hot gas bulging by controlling internal pressure. To form Ti-alloy and high strength steel tubular component with a large expansion ratio, it is important to increase the deforming temperature and the internal pressure. Vadillo [13] and Neugebauer [14] studied the high strength steel forming process at elevated temperature and summarized the applications of high strength steel parts prepared by tube gas forming. Maeno [15] fabricated an ultra-high strength steel hollow part by filling pressurized air high temperature deforming. Elsenheimer and Groche [16] designed a hot tube bulging equipment to test stress–strain curves of the high strength steel tube at elevated temperature and the maximal gas pressure of the equipment could be 35 MPa.

On the other hand, titanium and its alloys are found extensive applications including aerospace, marine, chemical, and medical industries due to their excellent properties such as good high temperature performance, high specific strength, good creep resistance, biocompatibility, and good corrosion resistance [17]. Especially, there has been paid much applicable attention for complicated shaped components of titanium alloy for aerospace field, e.g. the blade of engine, air-inlet system, and hydraulic control system [18, 19]. However, due to its poor formability, high springback, and strong deforming resistance, it is very difficult to fabricate such components of titanium alloy using traditional cold-pressing methods at room temperature [20, 21]. In addition, the superplastic forming is an effective way to obtain complicated parts in one-step, and it can reduce the cost for manufacturing Ti alloy [18, 22, 23]. Nevertheless, the disadvantages of localized thinning, expensive microstructure refining processing, low productive efficiency, and high deforming temperature in superplastic forming have been the bottleneck for actual processing of Ti alloy.

Based on the above discussions and previous research achievements on high pressure tube gas forming of Ti-alloy components [24–26], the deforming behavior of Ti-3Al-2.5 V tubular components with 50 % expansion ratio was investigated by considering the advantages of hydroforming and warm processing. To obtain uniform thickness distribution for this kind of hard-to-deform alloy, a two-stage loading path during deforming process was well designed. In particular, the effect of various axial feeding lengths on the microstructure and mechanical properties of Ti-3Al-2.5 V alloy during processing has been comprehensively studied, which will help to better design and fabricate Ti alloy tubular component using the hot tube gas forming technique.

2 Experimental procedures

2.1 Materials

The as-received material used in this study is Ti-3Al-2.5 V titanium alloy tube with an outer diameter of 40 mm and nominal thickness of 2 mm. The as-received tubes are produced through cold rolling method at room temperature and annealed at 680 °C for 2 h. This alloy is a near-α phase titanium alloy evolved from Ti-6Al-4 V. The α-Ti alloy possesses a hexagonal structure and the β-Ti alloy possesses a body-centered cubic structure. Figure 1a shows the microstructure of the as-received tube. The bright contrast is the α phase and the dark area is the β phase. Most of the α phase grains exhibit equiaxed characteristics. Uniaxial tensile tests were carried out to evaluate the mechanical properties of as-received tubes at 800 °C. The as-received tube samples were machined along the tube axial direction using the low-speed wire electrical discharge machine (WEDM). The true stress–strain curves are shown in Fig. 1b. The maximal true strains are 0.45, 0.56, and 0.77 when initial strain rates are 10^{-1} s^{-1}, 10^{-2} s^{-1}, and 10^{-3} s^{-1}, respectively. The tensile result shows that it is possible to form a tubular component with 50 % expansion ratio with feeding at 800 °C.

2.2 High pressure tube gas forming

Figure 2 shows the schematic diagram of high pressure tube gas forming. Similar to the tube hydroforming, the entire forming process can be divided into four stages. During the first stage, a tube is placed into the heated tool and sealed by punches. Meanwhile, the titanium tube is heated to deforming temperature. The first stage takes about 500 s. For an annealed Ti-3Al-2.5 V tube, the effects on grain size can be ignored because of short heating time and low temperature. At the second stage, using low internal pressure P_1, the punch pushes the materials of tube into the die cavity along axial direction. Wrinkles are formed in the die cavity because of the axial stress. Most of the materials of the tube are used to form the wrinkle and store in the wrinkle. Subsequently, at the third stage, the tubular component is calibrated by the improved internal pressure. The wrinkle is flattened by the internal pressure. Since the materials were store in the wrinkle during the second stage, the thinning ratio of the component is smaller than that of the tubular component formed without axial feeding. At last stage, the formed tubal component is cooled by water.

The forming tests are carried out on the platform developed by the Engineering Research Center of hydroforming in Harbin Institute of Technology (ERCH/HIT). The experimental device is shown in Fig. 3a, including the press, dies, heating equipment, and high pressure gas system. The constant temperature of the tool can be obtained by the synergetic control of a water cooling system and electromagnetic induction heating equipment, with a 5 °C temperature error. Three through-holes were designed in the molds. Three thermocouples were put into the holes to measure the out temperature of the tubes. The pressurized Argon with a maximal pressure of 70 MPa is used in the test, supplied by the high pressure gas system. All of the forming setup is assembled on 3150KN hydraulic machine. Boron nitride powder is sprayed onto the surface of the tube uniformly as lubricant and antioxidant. The designed outer contour with 50 % expansion ratio of the tube

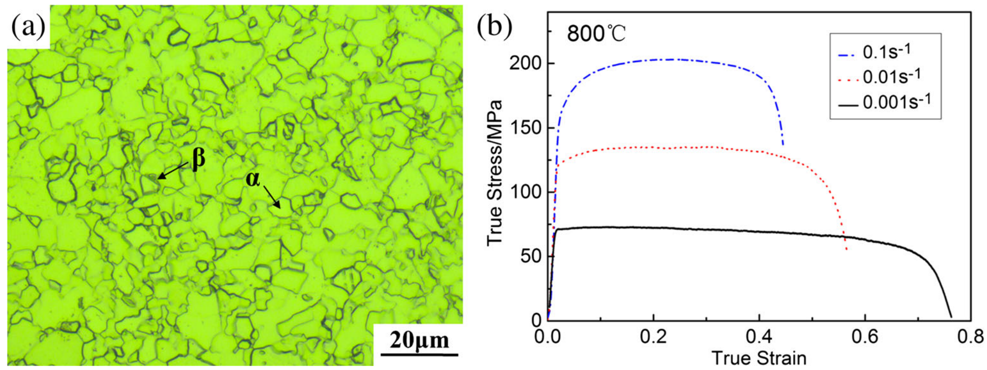

Fig. 1 **a** Microstructure of the as-received Ti-3Al-2.5 V tube. **b** True stress–strain curve at 800 °C of as-received Ti-3Al-2.5 V tube

component is shown in Fig. 3b. Welf-Guntram Drosse [27] designed an innovative measuring instrument to determine the gas temperature curve, and the result shows that the cold gas will cool the heated tube. In this paper, some steel filler was put inside the tube, which used to reduce the volume of the tube cavity and preheat the argon gas.

The most important parameters in tube hydroforming process are internal pressure and axial force loading paths. In hydroforming, some researchers [28, 29] investigated the effect of internal pressure and axial feeding loading paths on qualities of components. Apparently, the loading path of high pressure tube gas forming is different from the one in hydroforming. In this paper, a two-stage loading path is proposed, as shown in Fig. 4. During the first 20 s, two ends of the tube are deformed and sealed by the axial feeding with a length of 5 mm. During the period from 20 to 220 s, the internal pressure is supplied as relatively low pressure (5 MPa) and the two punches push the materials into die cavity with 0.1 mm/s, which is defined as the first feeding stage. During the period from 220 to 320 s, called the second feeding stage, the punches feed materials with 0.2 mm/s and the internal pressure is adjusted to 7 MPa. After the feeding stage, the internal pressure was increased to 30 MPa to calibrate the tubular part. The whole calibration stage takes about 180 s.

In hydroforming, the feeding ratio is an important parameter. The ratio between the actual axial feeding length and the theoretical axial feeding length is called the feeding ratio. It is usually to estimate the theoretical feeding length following the principle of volume and thickness constancy. In this paper, the theoretical axial feeding length is 45 mm. Following the loading path in Fig. 4, different tubular components were formed by feeding 25, 35, and 45 mm at 800 °C to study the effect of on the formed components, whose axial feeding ratios are 56 %, 78 %, and 100 %, respectively. A tubular component is deeded to comparison, which formed by constant internal pressure of 10 MPa with feeding 0 mm. Then, the various components were studied to get a better axial feeding ratio.

2.3 Microstructure and mechanical property

The microstructures of the specimens were observed by optical microscopic (OM) and electron backscattering diffraction (EBSD). The EBSD measurements were carried out on a FEI Quanta 200 FEG scanning electron microscope, and the analysis was performed by the software TSL OIM 5.31. Specimens were prepared by the standard grinding and electrochemical polishing (chemical composition 60 % carbinol+ 34 % butarol+6 % perchloric acid, temperature −20 °C, the electric current 0.89A and time 1 min). The EBSD data were collected with a step size of 1.2 mm and 1000 magnification. Specimens of metallographic observation were etched by corrosive solution (2 % HF+2 % HNO_3+96 % H_2O). The uniaxial tensile specimens were cut from the center of

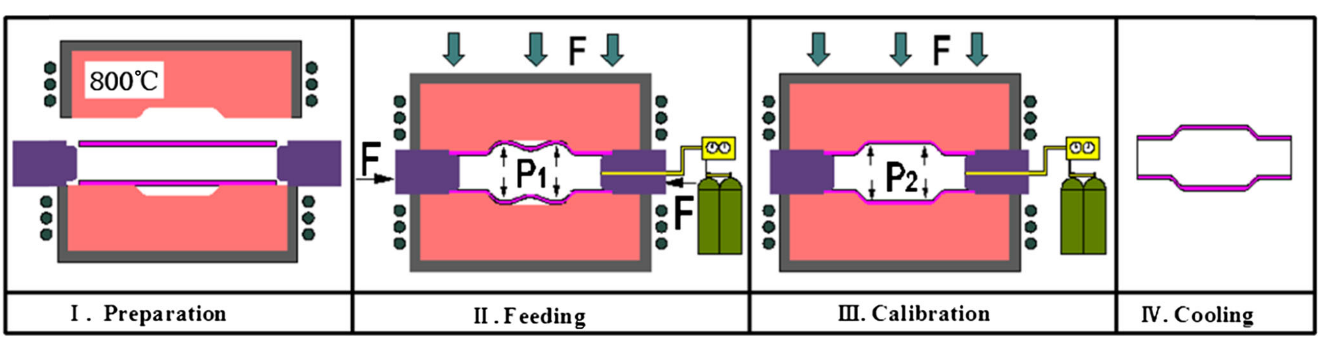

Fig. 2 Schematic diagram of high pressure gas forming

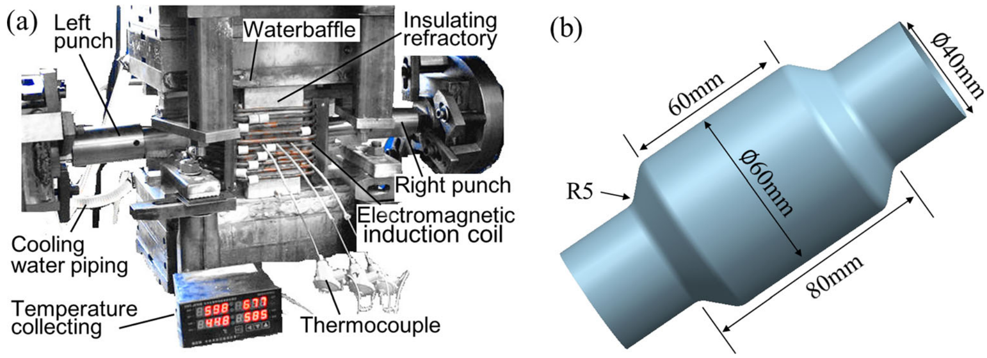

Fig. 3 Experimental conditions: **a** the experimental platform of high pressure tube gas forming, **b** the designed model of a tubular component with large expansion ratio

components along the axial direction and ground to obtain uniform thickness. Then, uniaxial tensile tests at room temperature with an initial strain rate of 0.001 s^{-1} were carried out to evaluate the mechanical properties of tubes formed by different technological parameters.

3 Discussion and result

3.1 Thickness distribution

The large expansion tubes formed with different axial feeding lengths are shown in Fig. 5. The wall thickness distributions are investigated to evaluate the effect of different axial feeding lengths on forming ability of components. The thinning ratio distribution along the axial position is shown in Fig. 6a. For the convenience of discussion, the component is divided into three zones, i.e., the feeding zone (zone A), transition zone (zone B), and bulging zone (zone C), respectively. With the increasing of the axial feeding, one can see the average thinning ratio of zone C decreases significantly. The average thinning ratios of zone C are 34.75 %, 24.29 %, 14.28 %, and 6.29 % when the theoretical feeding ratios are 0 %, 56 %, 78 %, and 100 %, respectively.

It is also of interest to note that the thinnest positions of tubular components change with increasing of feeding distance. For the tubular components with a feeding ratio of 0 %, the minimal wall thickness exists at the point of tangency near filleted corner. Chen [30] and Hwang [31] have investigated the effect factors of the thickness distribution: (1) the deforming stress of the material at the corner is smaller than that at the point of tangency; (2) the effect of the friction between tube and die at straight wall on the thickness distribution. With the increasing of feeding ratio, the plastic deformation of the alloy takes place along the circumferential direction. When the feeding ratio is 56 %, the thinnest position shifts to the center of the tube because the feeding material mainly accumulates at the corner position at this case, rather than the center. With further increasing the feeding ratio to 78 % and 100 %, the minimal wall thickness returns to near

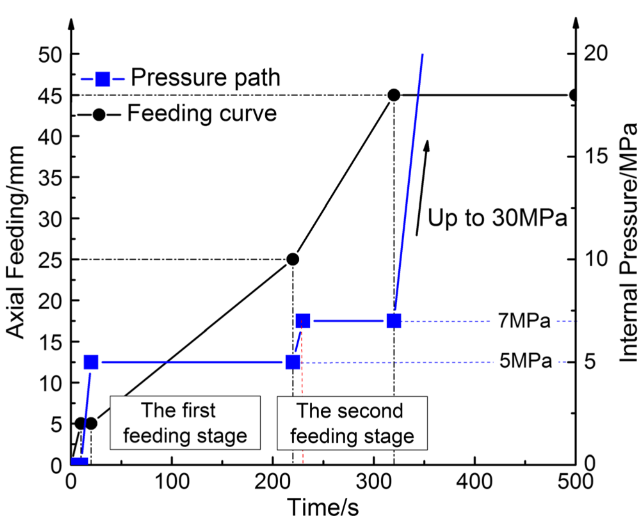

Fig. 4 Two stage axial feeding and pressure paths used for experiments

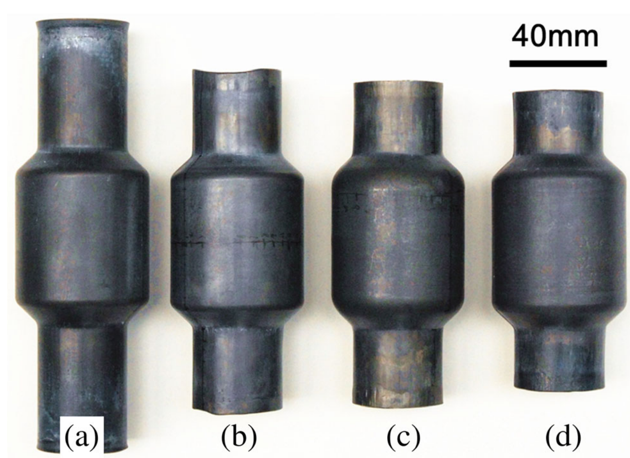

Fig. 5 Tubular components formed by high pressure gas tube forming with different axial feeding ratios: **a** feeding ratio 0 %, bulged with constant internal pressure 10 MPa, **b** feeding ratio 56 %, formed following path loading and calibrated after axial feeding 25 mm, **c** feeding ratio 78 %, formed following path loading and calibrated after axial feeding 35 mm, **d** feeding ratio 100 %, formed following path loading and calibrated after axial feeding 45 mm

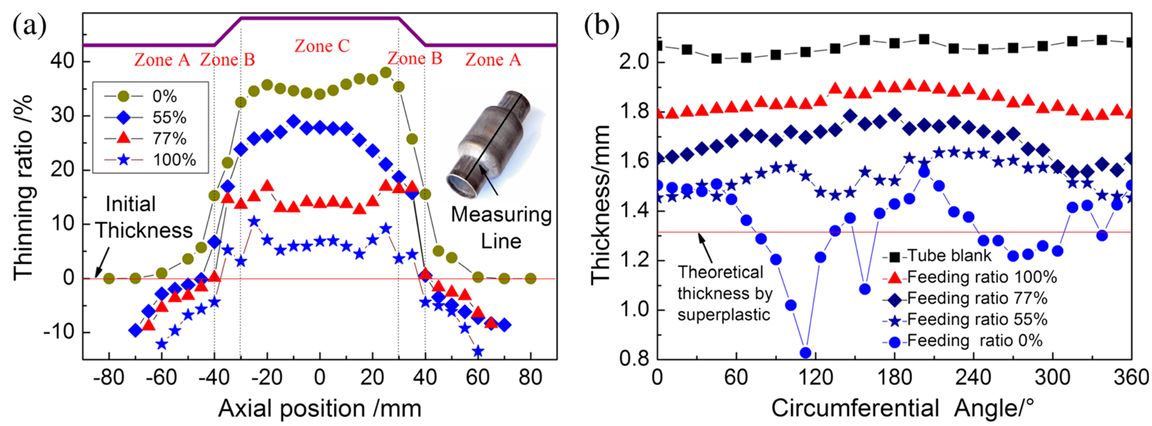

Fig. 6 Thickness distribution of tubular components formed by different technological parameters. **a** Thickness distribution along axial direction. **b** Thickness distribution along circumferential direction at the thinnest position of tubular component along axial direction

the filleted corner, because the accumulated materials are adequate to prevent the thickness reducing of tube center.

Moreover, in order to reveal the comprehensive deforming behavior of this Ti alloy with different feedings, the circumferential thickness distributions at the minimal thickness position along axial direction of the tubular components are further investigated, as shown in Fig. 6b. The wall thickness of the as-received tube is in the range of 2.0–2.1 mm, and the straight line with the thickness value around 1.3 mm in Fig. 6b describes the circumferential thickness of the tubular component formed by theoretical superplastic forming without feeding, which is regarded as a reference. Obviously, with the increasing of axial feeding, the circumferential thickness distribution becomes uniform, i.e., the maximal thinning ratios are 58.7 %, 27.3 %, 22.1 %, and 10.9 % for the cases of axial theoretical feeding ratios of 0 %, 56 %, 78 %, and 100 %, respectively.

3.2 Microstructure after bulging

Figure 7 depicts EBSD results of the as-received tube. Figure 7a shows the microstructure and orientation distribution of α phase for the as-received tube while β phase is so scarce to analyze. The chart of the grain size distribution is shown in Fig. 7b. The mean size of equiaxed grains is 12.8 μm. Small grains with numerous low angle grain boundaries (LGBS, 2°–15°) existed along large grains. These small grains are connected with each other, which is termed as "necklace structure", a common product of the thermo-mechanical processing for two-phase Ti-alloys [32–34].

In order to evaluate the effect of axial feeding on microstructure and mechanical properties, the microstructure of tubular components formed by different technological parameters was observed, as shown in Fig. 8. The sampling points are illustrated. The microstructure (including grain boundaries) and the orientation distribution were presented. True strains along axial position, circumferential position, and thickness position are also shown. Figure 10 shows the distribution of grains size for tubular components formed by different technological parameters. Grain sizes are significantly different although the equivalent strains of different samples are almost equivalent.

Figure 8a shows the microstructure and orientation distribution of the tubular component formed without axial feeding. Tiny recrystallized grains (<5 μm) are presented in a large number (Fig. 9a). The mean size is 7.5 μm. When the feeding ratio is 56 %, the result is shown in Fig. 8b. The microstructure

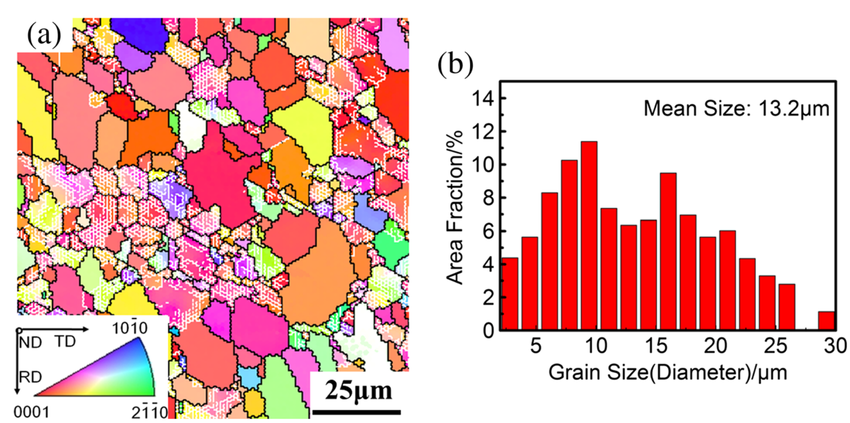

Fig. 7 The microstructure and orientation distribution of the as-received tube: **a** IPF map showing LGBS. In this map, TD is the axial direction, RD is the circumferential direction, ND is the thickness direction. *White contours* represent low angle grain boundaries (2°–15°). (**b**) Chart of the grain size distribution

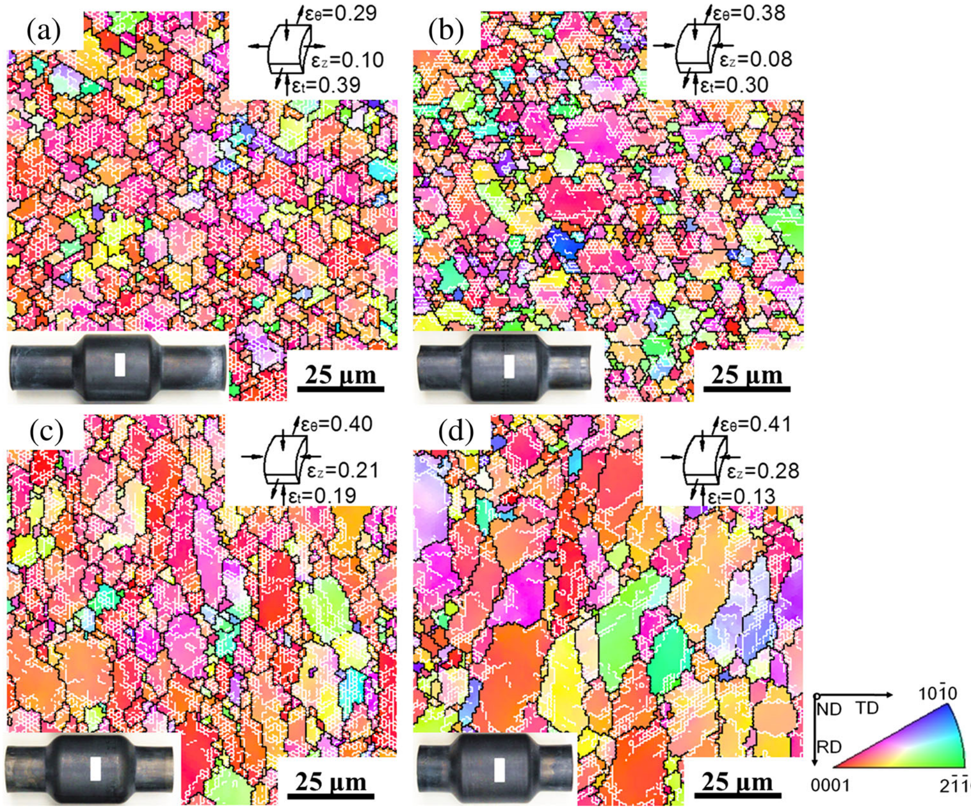

Fig. 8 The microstructure and strain state of tubular components formed by different schemes. In this map, TD is the axial direction, RD the is circumferential direction, ND is the thickness direction, and *white contours* represent the low angle grain boundary (2°–15°). **a** feeding ratio 0 %, **b** feeding ratio 56 %, **c** feeding ratio 78 %, **d** feeding ratio 100 %

with uniform tiny recrystallized grains is presented. There are a mass of LGBS in coarse grains, which are caused by large plastic deformation. And plenty of tiny grains appear along boundary of original grains. Small "new" grains do not grow.

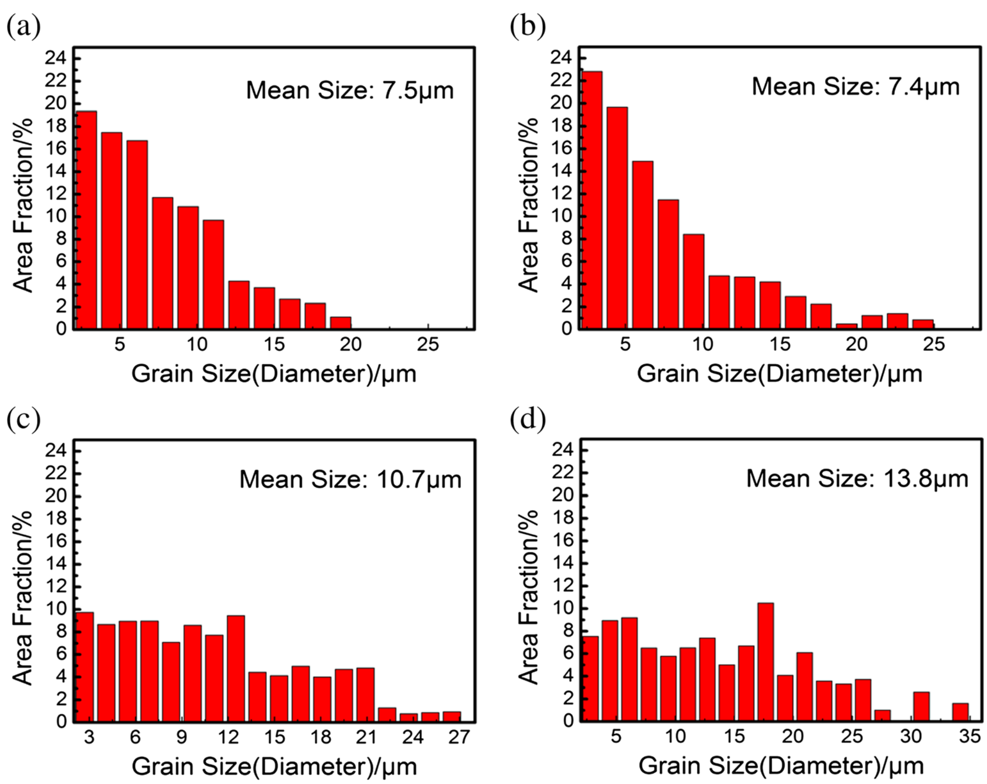

Fig. 9 Chart of the grain size distribution: **a** feeding ratio 0 %, **b** feeding ratio 56 %, **c** feeding ratio 78 %, **d** feeding ratio 100 %

Figure 9b shows that the proportion of small grains (<5.0 μm) is about 45 %. The mean size of grains is 7.4 μm. As feeding length increasing, the mean size of grains becomes larger and the proportion of recrystallized grains reduces significantly. Figure 8c shows the microstructure of tubular components formed with a feeding ratio 78 %. The grains were elongated along circumferential position because the tube material was compressed along the axial position and stretched along circumferential position. The grain size distribution is presented in Fig. 9c, as like the original tube. This can be interpreted in a dynamic equilibrium between refining grains by recrystallization and coarsening grains normally at elevated temperature. As which can be seen from Fig. 8d, the grains are elongated more severely when the feeding ratio is 100 %. As shown in Fig. 9d, tiny recrystallized grains and abnormal coarse grains (>15 μm) are both plentiful. The coarsening grains are produced because the grains are growing normally in hot working and the small deformation can't break down them. The mean grain is 13.8 μm. Through analysis above, we can get the speculation that the microstructure of tubular component depends on the technological parameters (axial feeding distance, feeding speed, strain rate, heat treatment time after deformation, the plastic deformation during the calibration stage, etc.).

3.3 Mechanical properties

Tensile tests are carried out to evaluate the mechanical properties of tube gas forming processed specimens. Figure 10 presents the engineering tensile stress–strain curves at room temperature. The position of specimens on the tube component is illustrated. The original tube has the tensile strength of 643 MPa and elongation of 24.6 %. In the case of the tubular component without feeding, a slightly decrease for the strength of the material can be seen, although it has relatively

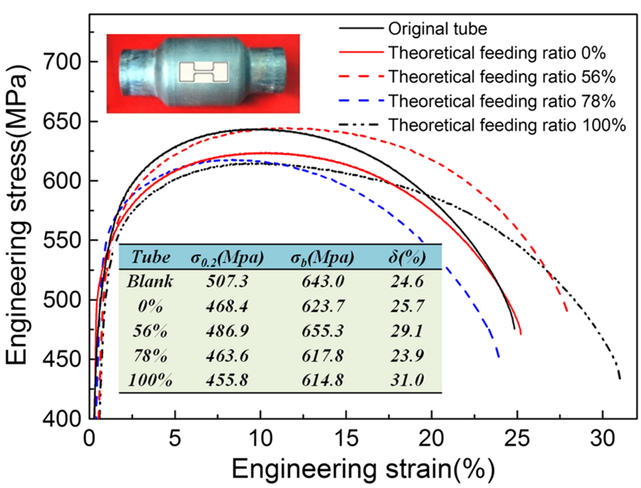

Tube	$\sigma_{0.2}$(Mpa)	σ_b(Mpa)	δ(%)
Blank	507.3	643.0	24.6
0%	468.4	623.7	25.7
56%	486.9	655.3	29.1
78%	463.6	617.8	23.9
100%	455.8	614.8	31.0

Fig. 10 The result of engineering tensile stress–strain curve of formed tube in tensile text at room temperature

smaller grain. The decreasing of strength is mainly caused by the internal defects, i.e., micro-sized cavitation in the tube after severe deformation [17]. When the feeding ratio increases to 56 %, the tensile strength is even higher than the original tube because of grain refinement effect, which follows the Hall–Petch relationship. Moreover, a more compacted microstructure (Fig. 8b), namely fewer internal defects caused by the axial feeding, also contributes to excellent mechanical performance. For larger feeding ratios of 78 % and 100 %, the grains become coarser. Therefore, both of the yielding strength ($\sigma_{0.2}$) and the tensile strength (σ_b) decrease. However, the lowest tensile strength can be 614.8 MPa when the feeding ratio is 100 %, which is similar to the original tube.

4 Conclusions

Compared with conventional hydroforming process, tube gas forming at elevated temperature is especially suitable for the alloys with high strength, high springback, and poor formability at room temperature. The Ti-3Al-2.5 V titanium alloy tubular components with 50 % expansion rate are formed by tube gas forming using different technological parameters. The deforming behavior, microstructure, and mechanical properties of component are investigated. The following conclusions are drawn from this work:

1. At 800 °C, the tensile strength of Ti-3Al-2.5 V is sensitive to the strain rate. Based on this, a two-stage loading path is adopted. At the first feeding stage, low internal pressure and low feeding speed are used to obtain a uniform deformation. At the second feeding stage, the internal pressure is increased to prevent dead winkles, while the feeding speed is also increased to improve the thinning of alloys on the wrinkle peak.
2. Without axial feeding, multiple necking occurs along the cross section of the component, which results in serious non-uniform thickness distribution. With the increasing of axial feeding, the maximal thickness thinning of component becomes smaller and the thickness is much more uniform. For example, the maximal thickness thinning without feeding is 53.23 %, while they reduce to 29.17 % and 13.02 % when the feeding increases to 56 % and 100 %, respectively.
3. During the tube gas forming process, the microstructures of the alloys experience different futures and the microstructure such as the grain size and defects can be efficiently designed and controlled by selecting the axial feeding. In this work, when the feeding ratio is 56 %, the mean grain size is 7.4 μm, which is nearly half of 13.2 μm for the as-received alloy. With further increasing of the feeding ratio, the mean grain size of alloys becomes larger and the grains are typically elongated along the circumferential direction.

4. The tensile strength of the component with feeding of 56 % can be 655 MPa, which is higher than 624 MPa without feeding due to the reduction of internal defects. With further increasing of the feeding ratio, the tensile strength of the alloys slightly decreases. The tensile strengths of the deformed alloys are in the range of 615–655 MPa, similar to strength of 643 MPa for the original tube.

In summary, high pressure gas tube forming is proposed to fabricate complicated shaped components using hard-to-deform alloys efficiently. The feeding length has a great effect on the deforming behavior, microstructure, and mechanical property of obtained components. The components with uniform thickness distribution, small grain sizes, and excellent mechanical properties can be formed by synergetic effect of feeding and calibration by high internal pressure. In the future, the resistance heating and a higher gas pressure can be tried to reduce the forming time.

Acknowledgments This work was financially supported by program for changjiang scholars and Innovative Research Team in University (No.IRT1229).

References

1. Geiger M, Merklein M, Celeghini M, Haldenwanger H-G, Prier M (2003) Sheet and tube hydroforming at elevated temperatures [J]. Hydroforming Tubes Extr Sheet Met 3:259–278
2. Yuan SJ, Qi J, He Z (2006) An experimental investigation into the formability of hydroforming 5A02 Al-tubes at elevated temperature [J]. J Mater Process Technol 177:680–683
3. Krajewski PE, Schroth JK (2007) Overview of quick plastic forming technology. Mater Sci Forum 551:1–11
4. Boissiere R, Terzi S, Blandin JJ, Salvo L (2008) Quick-plastic forming: similarities and differences with super-plastic forming. Proceedings of the 6th EUROSPF Conference, Euro SPF08, Carcassonne. pp. 1–8
5. Neugebauer R, Altan T, Geiger M, Kleiner M, Sterzing A (2006) Sheet metal forming at elevated temperatures. Ann CIRP 2(55): 793–816
6. Dykstra B (2001) Hot metal gas forming—the next generation process for manufacturing vehicle structural components. SAE Tech Pap 1:4271–3088
7. Wu X (2007) Non-steady-state creep behavior in tube gas forming. J Mater Eng Perform 16(4):418–431
8. Kim WJ, Kim WY, Kim HK (2010) Hot-Air forming of Al-Mg-Cr alloy and prediction of failure based on zener-holloman parameter. Met Mater Int 6(16):895–903
9. Amborn P, Kipry K, Groche P (2006) Elsenheimer. HEATforming als Weiterentwicklung des IHU an der Schwelle zur Massivumformung, Proc. of the 9th Forming Colloquium Darmstadt. 89–103
10. Maeno T, Mori K, Unou C (2011) Optimisation of condition in hot gas bulging of aluminium alloy tube using resistance heating set into dies. Key Eng Mater 473:69–74
11. Maeno T, Ken-ichiro M, Kouji F (2014) Hot gas bulging of sealed aluminium alloy tube using resistance Heating. Manuf Rev 1(5):1–7
12. Maeno T, Mori K, Unou C (2014) Improvement of die filling by prevention of temperature drop in gas forming of aluminium alloy tube using air filled into sealed tube and resistance heating. Procedia Eng 81:2237–2242
13. Vadillo L, Pérez I, Hori I, Zarazua JI, Mangas A, San JJ, Paar U (2010) Gas forming of boron steel tubes at low pressure-applasting. Steel Res Int 81(9):552–555
14. Neugebauer R, Schieck F (2010) Active media-based form hardening of tubes and profiles. Prod Eng 4(4):385–390
15. Maeno T, Mori K, Adachi K (2014) Gas forming of ultra-high strength steel hollow part using air filled into sealed tube and resistance heating. J Mater Process Technol 214:97–105
16. Elsenheimer D, Groche P (2009) Determination of material properties for hot hydroforming. Prod Eng Res Dev 3:165–174
17. Gollapudi S, Charit I, Murty KL (2008) Creep mechanisms in Ti–3Al–2.5V alloy tubing deformed under closed-end internal gas pressurization. Acta Mater 56:2406–2419
18. Barnes AJ (2007) Superplastic forming 40 years and still growing. J Mater Eng Perform 16:440–454
19. Brewer WD, Keith Bird R, Wallace TA (1998) Titanium alloys and processing for high speed aircraft. Mater Sci Eng A 243:299–304
20. Zhan M, Huang T, Zhang PP, Yang H (2014) Variation of young's modulus of high-strength ta18 tubes and its effects on forming quality of tubes by numerical control bending. Mater Des 53:809–815
21. Zhu-bin H, Bu-gang T, Chang-yong C, Zhi-biao W, Kai-lun Z, Shi-jian Y (2012) Mechanical properties and formability of TA2 extruded tube for hot metal gas forming at elevated temperature. Trans Nonferrous Met Soc China 22:479–484
22. Xun YW, Tan MJ (2000) Applications of superplastic forming and diffusion bonding to hollow engine blades. J Mater Process Technol 99:80–85
23. Ghosh AK, Hamiltion CH (1979) Mechanical behavior and hardening characteristics of a superplastic Ti-6Al-4V alloy. Metall Trans A 6:700
24. Liu Gang W, Yong WJ-L, Wen-Da Z (2014) Progress on high pressure pneumatic forming and warm hydroforming of Titanium and Magnesium alloy tubular components. Mater Sci Forum 783–786:2456–2461
25. Liu G, Wang KH, Xu Y, Wang B, Yuan SJ (2013) An approach to improve thickness uniformity of TA15 tubular part formed by gas bulging process. Adv Mater Res 712–715:651–657
26. Gang L, Jianlong W, Kexin D, Zejun T (2014) High pressure pneumatic forming of Ti-3Al-2.5V titanium tubes in a square cross-sectional Die. Materials 7:5992–6009
27. Drossel W, Pierschel N, Paul A, Katzfuß K, Demuth R (2014) Determination of the active medium temperature in media based press hardening processes. J Manuf Sci Eng 136:021013
28. Hama T, Ohkubo T, Kurisu K, Fujimoto H, Takuda H (2006) Formability of tube hydroforming under various loading paths. J Mater Process Technol 177:676–9
29. Kim S, Kim Y (2002) Analytical study of tube hydroforming. J Mater Process Technol 128(1–3):232–9
30. Yang C, Ngaile G (2008) Analytical model for planar tube hydroforming: Prediction of formed shape, corner fill, wall thinning, and forming pressure. Int J Mech Sci 50:1263–1279
31. Hwang Y-M, Chen W-C (2005) Analysis of tube hydroforming in a squarecross-sectional die. Int J Plast 21:1815–1833
32. Lin P, Feng A, Yuan S, Li G, Shen J (2013) Microstructure and texture evolution of a near-atitanium alloy during hot deformation. Mater Sci Eng A 563:16–20
33. Thomas RB, Semiatin SL (2002) The origins of heterogeneous deformation during primary hot working of Ti–6Al–4V. Int J Plast 18:1165–1189
34. He D, Zhu JC, Lai ZH, Liu Y, Yang XW (2013) An experimental study of deformation mechanism and microstructure evolution during hot deformation of Ti–6Al–2Zr–1Mo–1V alloy. Mater Des 46: 38–48